

COSMOLOGY WITH GRAVITATIONAL WAVE/FAST RADIO BURST ASSOCIATIONS

JUN-JIE WEI,¹ XUE-FENG WU,^{1,2} AND HE GAO³

¹Purple Mountain Observatory, Chinese Academy of Sciences, Nanjing 210034, China; jjwei@pmo.ac.cn

²School of Astronomy and Space Science, University of Science and Technology of China, Hefei, Anhui 230026, China

³Department of Astronomy, Beijing Normal University, Beijing 100875, China

Draft version March 27, 2022

ABSTRACT

Recently, some theoretical models predicted that a small fraction of fast radio bursts (FRBs) could be associated with gravitational waves (GWs). In this work, we discuss the possibility of using GW/FRB association systems, if commonly detected in the future, as a complementary cosmic probe. We propose that upgraded standard sirens can be constructed from the joint measurements of luminosity distances D_L derived from GWs and dispersion measures DM_{IGM} derived from FRBs (i.e., the combination $D_L \cdot DM_{\text{IGM}}$). Moreover, unlike the traditional standard-siren approach (i.e., the D_L method) and the DM_{IGM} method that rely on the optimization of the Hubble constant H_0 , this $D_L \cdot DM_{\text{IGM}}$ method has the advantage of being independent of H_0 . Through Monte Carlo simulations, we prove that the $D_L \cdot DM_{\text{IGM}}$ method is more effective to constrain cosmological parameters than D_L or DM_{IGM} separately, and enables us to achieve accurate multimessenger cosmology from around 100 GW/FRB systems. Additionally, even if GW/FRB associations are not exist, the methodology developed here can still be applied to those GWs and FRBs that occur at the same redshifts.

Subject headings: cosmological parameters — gravitational waves — intergalactic medium

1. INTRODUCTION

With the rapid development of modern astronomical technology, the research of cosmology has been promoted into the age of precision. Cosmological parameters can now be inferred precisely from the observations of various electromagnetic (EM) waves, such as cosmic microwave background anisotropies (Hinshaw et al. 2013; Planck Collaboration et al. 2016), Type Ia supernovae (Perlmutter et al. 1998; Riess et al. 1998), baryon acoustic oscillations (Beutler et al. 2011; Anderson et al. 2012), and so on.

In addition to the traditional EM methods, the observation of gravitational waves (GWs) also provides an alternative probe for cosmological studies. Due to the fact that the waveform signal of GWs from inspiralling and merging compact binaries encodes the luminosity distance (D_L) information, GWs can be considered as standard sirens (Schutz 1986). The greatest advantage of GW standard sirens is that the distance calibration is independent of any other cosmic distance ladders (i.e., it is self-calibrating). Thus, detections of GW together with their EM counterparts providing the source redshifts, could give the D_L - z relation for measuring the cosmic expansion (Holz & Hughes 2005; Zhao et al. 2011). Especially, GW signals from binary neutron stars (NSs) or black hole (BH)-NS mergers are promising for conducting cosmography, since these merging systems are expected to be accompanied by some detectable EM signals, e.g., fast radio bursts (FRBs), short Gamma-Ray Bursts (GRBs), or kilonovae/mergernovae (see Fernández & Metzger 2016 for review). In the past, several works have discussed the possibility of GWs as standard sirens and showed that with hundreds of simulated GW events they can determine the cosmological parameters with accuracies comparable to traditional probes (e.g., Holz & Hughes 2005; Zhao et al. 2011; Del Pozzo 2012; Cai & Yang 2017; Del Pozzo et al. 2017). Very recently, the coincident detection of a gravitational-wave event GW170817 with EM counterparts (e.g., a GRB 170817A or a macronova) from a binary NS merger has

formally opened the new era of multimessenger astronomy (Abbott et al. 2017a; Coulter et al. 2017; Goldstein et al. 2017; Savchenko et al. 2017). Using this first truly GW/EM association, Abbott et al. (2017b) performed a standard siren measurement of the Hubble constant H_0 .

On the other hand, FRBs are a new mysterious class of millisecond-duration radio transients (Lorimer et al. 2007; Thornton et al. 2013). These objects have anomalously large dispersion measures (DMs), suggesting a cosmological origin for FRBs. The DM is defined as the integral of the electron number density along the propagation path from the source to the observer. Since the observed DMs of FRBs contain important information on the cosmological distance they have traveled, one may combine the DM and z information to probe cosmology if more FRBs with known redshifts can be detected (Deng & Zhang 2014; Gao et al. 2014; Zheng et al. 2014; Zhou et al. 2014; Yang & Zhang 2016).

Regarding to the physical origins, some studies suggested that mergers of double NSs (Totani 2013; Wang et al. 2016; Yamasaki et al. 2017), of BH-NS (Mingarelli et al. 2015), or even of charged BHs (Zhang 2016), could be responsible for FRBs. Particularly, Wang et al. (2016) showed that an FRB could originate from the magnetic interaction between binary NSs during their final inspiral within the framework of the unipolar inductor model. The NS-NS merger has been recently confirmed as the progenitor system of GW170817 and GRB 170817A (Abbott et al. 2017a; Goldstein et al. 2017; Savchenko et al. 2017). If FRBs can indeed be interpreted with the NS-NS merger model, it would be expected to detect possible associations of FRBs with short GRBs and GW events in the future (Wang et al. 2016). Alternatively, Zhang (2016) proposed that if at least one of the two merging BHs carries a certain amount of charge, the inspiral process would drive a global magnetic dipole. The rapid evolution of the magnetic moment of the BH-BH system would lead to a magnetospheric outflow with an increasing wind power, which may produce an FRB and even a short GRB depending on the value of the charge. The detection of an FRB associated with

future NS–NS (or BH–BH) merger GW events would verify the NS–NS (or BH–BH) merger model.

In this work, we show that if such GW/FRB association systems are commonly detected in the future, ‘upgraded standard sirens’ could be constructed from the combination of D_L derived from GWs and DM derived from FRBs, independent of the Hubble constant H_0 . We explore its use to constrain the cosmological parameters in view of the large samples of GWs and FRBs to be found in the third-generation GW interferometric detectors such as the Einstein Telescope (ET) and the upcoming radio transient surveys such as the Square Kilometer Array.

2. GW/FRB ASSOCIATIONS AS UPGRADED STANDARD SIRENS

2.1. Luminosity distances from gravitational waves

The third-generation GW ground-based detectors such as the ET, with ultra high sensitivity, would significantly improve the detection rate of the GW events. The ET is designed to be ten times more sensitive than the current advanced laser interferometric detectors, covering the frequency range of $1 - 10^4$ Hz. It has three interferometers with 10 km arm lengths and 60° opening angles, arranged in an equilateral triangle. Here, we present an overview of using GWs as standard sirens in the potential ET observations (see also Cai et al. 2017 for a recent review). Throughout we use units $G = c = 1$.

The amplitude of the GW depends on the chirp mass and the luminosity distance D_L . Because the chirp mass can already be obtained from GW signal’s phasing, D_L can be extracted from the amplitude of waveform. In the transverse-traceless gauge, the strain $h(t)$ is the linear combination of the two components of the GW’s tensor (i.e., h_+ and h_\times),

$$h(t) = F_+(\theta, \phi, \psi)h_+(t) + F_\times(\theta, \phi, \psi)h_\times(t), \quad (1)$$

where F_+ and F_\times are the beam-pattern functions, (θ, ϕ) are angles describing the location of the source relative to the detector, and ψ denotes the polarization angle. The corresponding antenna pattern functions of one of the interferometers in the ET are (Zhao et al. 2011)

$$\begin{aligned} F_+^{(1)}(\theta, \phi, \psi) &= \frac{\sqrt{3}}{2} \left[\frac{1}{2} (1 + \cos^2(\theta)) \cos(2\phi) \cos(2\psi) \right. \\ &\quad \left. - \cos(\theta) \sin(2\phi) \sin(2\psi) \right], \\ F_\times^{(1)}(\theta, \phi, \psi) &= \frac{\sqrt{3}}{2} \left[\frac{1}{2} (1 + \cos^2(\theta)) \cos(2\phi) \sin(2\psi) \right. \\ &\quad \left. + \cos(\theta) \sin(2\phi) \cos(2\psi) \right]. \end{aligned} \quad (2)$$

The other two interferometers’ antenna pattern functions can be derived from Equation (2), since the interferometers have 60° with each other. That is to say, $F_{+, \times}^{(2)}(\theta, \phi, \psi) = F_{+, \times}^{(1)}(\theta, \phi + 2\pi/3, \psi)$ and $F_{+, \times}^{(3)}(\theta, \phi, \psi) = F_{+, \times}^{(1)}(\theta, \phi + 4\pi/3, \psi)$.

In this paper, we focus on the GW signals produced by the merger of binary systems. Considering a merging binary with component masses m_1 and m_2 , the chirp mass is defined to be $\mathcal{M}_c = M\eta^{3/5}$, where $M = m_1 + m_2$ is the total mass, and $\eta = m_1 m_2 / M^2$ represents the symmetric mass ratio. For a GW source locating at cosmological distance with redshift z , the observed chirp mass is given by $\mathcal{M}_{c, \text{obs}} = (1+z)\mathcal{M}_{c, \text{phys}}$. Below, \mathcal{M}_c always refers to the observed chirp mass. Following Sathyaprakash & Schutz (2009) and Zhao et al. (2011), we apply the stationary phase approximation to calculate the

Fourier transform $\mathcal{H}(f)$ of the time domain waveform $h(t)$,

$$\mathcal{H}(f) = \mathcal{A} f^{-7/6} \exp \left[i \left(2\pi f t_0 - \pi/4 + 2\psi(f/2) - \varphi_{(2,0)} \right) \right], \quad (3)$$

where the constant t_0 is the epoch of the merger. The definitions of the functions ψ and $\varphi_{(2,0)}$ are presented in Zhao et al. (2011). The Fourier amplitude \mathcal{A} is given by

$$\begin{aligned} \mathcal{A} &= \frac{1}{D_L} \sqrt{F_+^2 (1 + \cos^2(\iota))^2 + 4F_\times^2 \cos^2(\iota)} \\ &\quad \times \sqrt{5\pi/96\pi^{-7/6} \mathcal{M}_c^{5/6}}, \end{aligned} \quad (4)$$

where ι denotes the angle of inclination of the binary’s orbital angular momentum with the line-of-sight, and

$$D_L(z) = \frac{1+z}{H_0} \int_0^z \frac{dz}{\sqrt{\Omega_m(1+z)^3 + (1-\Omega_m)(1+z)^{3(1+w)}}} \quad (5)$$

is the theoretical luminosity distance in the w CDM model. Note that averaging the Fisher matrix over the inclination ι and the polarization ψ with the constraint $\iota < 20^\circ$ is approximately equivalent to taking $\iota = 0$. Therefore, we only consider the simplified case of $\iota = 0$ and \mathcal{A} is independent of the polarization angle ψ (Cai & Yang 2017).

Given the waveform of GWs, we can compute the signal-to-noise ratio (SNR) of the GW detection. The combined SNR for the network of three independent ET interferometers is

$$\rho = \sqrt{\sum_{i=1}^3 \langle \mathcal{H}^{(i)}, \mathcal{H}^{(i)} \rangle}, \quad (6)$$

where the inner product is defined as

$$\langle a, b \rangle = 4 \int_{f_{\text{lower}}}^{f_{\text{upper}}} \frac{\tilde{a}(f)\tilde{b}^*(f) + \tilde{a}^*(f)\tilde{b}(f)}{2} \frac{df}{S_h(f)}, \quad (7)$$

where the superscript “ \sim ” stands for the Fourier transform of the corresponding function and $S_h(f)$ is the one-side noise power spectral density. We take the ET’s $S_h(f)$ to be the same as in Zhao et al. (2011). The upper cutoff frequency is assumed to be $f_{\text{upper}} = 2f_{\text{LSO}}$, where $f_{\text{LSO}} = 1/(6^{3/2}2\pi M_{\text{obs}})$ corresponds to the orbit frequency at the last stable orbit, and $M_{\text{obs}} = (1+z)M_{\text{phys}}$ is the observed total mass (Zhao et al. 2011). The lower cutoff frequency f_{lower} is fixed to be 1 Hz. The signal is identified as a GW event only when the ET interferometers have a network SNR of $\rho > 8.0$.

Using the Fisher information matrix, we can estimate the instrumental uncertainty on the measurement of D_L , which can be expressed as (Zhao et al. 2011)

$$\sigma_{D_L}^{\text{inst}} \simeq \sqrt{\left\langle \frac{\partial \mathcal{H}}{\partial D_L}, \frac{\partial \mathcal{H}}{\partial D_L} \right\rangle^{-1}}. \quad (8)$$

Assuming that the uncertainty of D_L is uncorrelated with the uncertainties of other GW parameters, we can get $\sigma_{D_L}^{\text{inst}} \simeq D_L/\rho$ due to $\mathcal{H} \propto d_L^{-1}$ (Cai & Yang 2017). Taking into account the maximal effect of the inclination ι on the SNR, we double the estimate of the error on D_L , i.e.,

$$\sigma_{D_L}^{\text{inst}} \simeq \frac{2D_L}{\rho}. \quad (9)$$

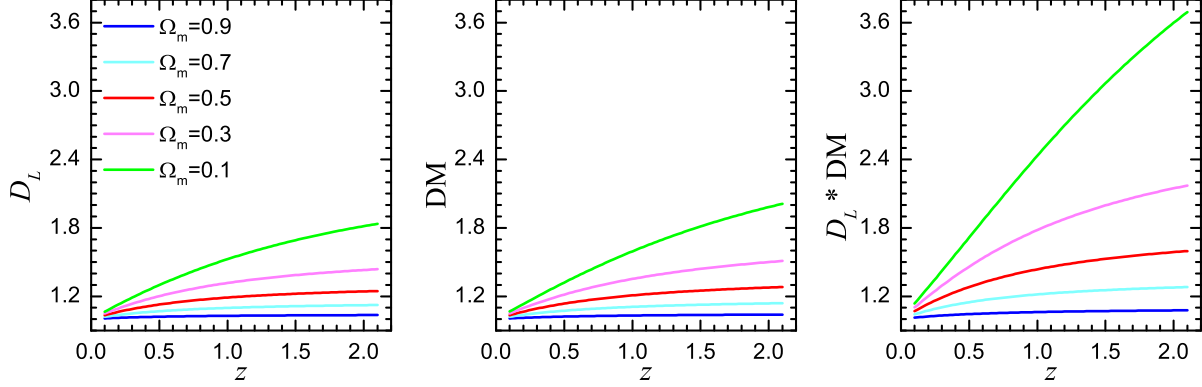


FIG. 1.— Sensitivity of three quantities (D_L , DM_{IGM} , and $D_L \cdot DM_{\text{IGM}}$) to the cosmological parameter. The flat Λ CDM model is adopted with five different Ω_m values: 0.1, 0.3, 0.5, 0.7, and 0.9. Each curve is obtained relative to the Einstein-de Sitter Universe.

We also add an additional error $\sigma_{D_L}^{\text{lens}}/D_L = 0.05z$ caused by the weak lensing. Thus, the total error on D_L is given by

$$\sigma_{D_L} = \sqrt{\left(\frac{2D_L}{\rho}\right)^2 + (0.05zD_L)^2}. \quad (10)$$

2.2. Dispersion measures from fast radio bursts

In principle, the observed DM of an FRB (DM_{obs} ; Deng & Zhang 2014; Gao et al. 2014; Yang & Zhang 2016)

$$DM_{\text{obs}} = DM_{\text{MW}} + DM_{\text{IGM}} + \frac{DM_{\text{HG}}}{1+z} \quad (11)$$

has contributions from the Milky Way (DM_{MW}), intergalactic medium (DM_{IGM}), and FRB host galaxy (DM_{HG}), respectively. Note that for a GRB-associated FRB, DM_{HG} has contributions from the host galaxy and the GRB blastwave. Among these terms, DM_{IGM} is the relevant one for cosmological studies. Considering local inhomogeneity of the intergalactic medium (IGM), we define the average DM of the IGM, which can be written as (Deng & Zhang 2014)

$$\langle DM_{\text{IGM}} \rangle = \frac{3H_0\Omega_b f_{\text{IGM}}}{8\pi m_p} \int_0^z \frac{\chi(z)(1+z)dz}{\sqrt{\Omega_m(1+z)^3 + (1-\Omega_m)(1+z)^{3(1+w)}}}, \quad (12)$$

where f_{IGM} is the fraction of baryon mass in the IGM, Ω_b is the current baryon mass fraction of the universe, $\chi(z) = (3/4)y_1\chi_{e,H}(z) + (1/8)y_2\chi_{e,He}(z)$, $y_1 \sim 1$ and $y_2 \simeq 4 - 3y_1 \sim 1$ are the hydrogen (H) and helium (He) mass fractions normalized to 3/4 and 1/4, respectively, and $\chi_{e,H}(z)$ and $\chi_{e,He}(z)$ are the ionization fractions for H and He, respectively. Since H and He are essentially fully ionized at $z < 6$ and at $z < 2$ separately (Fan et al. 2006; McQuinn et al. 2009), it is reasonable to take $\chi_{e,H}(z) = \chi_{e,He}(z) = 1$ for nearby FRBs ($z < 2$). One then has $\chi(z) \simeq 7/8$.

As long as DM_{obs} , DM_{MW} , and DM_{HG} can be precisely determined, one can infer the value of $\langle DM_{\text{IGM}} \rangle$ (see Equation (11)). Then, we can calculate the total uncertainty of $\langle DM_{\text{IGM}} \rangle$ using the expression

$$\sigma_{DM_{\text{IGM}}} = \left[\sigma_{\text{obs}}^2 + \sigma_{\text{MW}}^2 + \sigma_{\text{IGM}}^2 + \left(\frac{\sigma_{\text{HG}}}{1+z}\right)^2 \right]^{1/2}. \quad (13)$$

Following Gao et al. (2014), we investigate different contributions of the relevant uncertainties in Equation (13) below.

Up to FRB 180311, a total of 33 FRBs have been detected (Petroff et al. 2016). The measurements of DM_{obs} and the cor-

responding uncertainties for these 33 FRBs are available in the FRB catalogue¹. Here, we adopt an average of these values as the uncertainty of DM_{obs} , i.e., $\sigma_{\text{obs}} = 1.5 \text{ pc cm}^{-3}$. With the ATNF pulsar catalogue (Manchester et al. 2005)², we find that the average uncertainty of DM_{MW} for high Galactic latitude ($|b| > 10^\circ$) sources is about 10 pc cm^{-3} , and we adopt this value as σ_{MW} . To be conservative, we associate an uncertainty of $\sigma_{\text{IGM}} = 100 \text{ pc cm}^{-3}$ to DM_{IGM} , as Yang & Zhang (2016) did in their treatment, with the hope that such a large uncertainty could account for the IGM inhomogeneity effect. On the basis of the DM uncertainty of the Milky Way, one may deduce that the uncertainty of DM_{HG} could be from tens to hundreds of pc cm^{-3} . In addition, Gao et al. (2014) showed that the resulting constraints on cosmological parameters are not very sensitive to the value of σ_{HG} , since σ_{HG} becomes less significant at high redshifts due to the $(1+z)$ factor. Here we adopt $\sigma_{\text{HG}} = 30 \text{ pc cm}^{-3}$.

2.3. The combination of D_L and DM

If FRBs are confirmed to be associated with GW events, the combination of D_L measurements of GWs and DM measurements of FRBs could provide upgraded standard sirens to study cosmology. From Equations (5) and (12), we can see that the Hubble constant H_0 cancels out when we multiply D_L by DM_{IGM} , so the constraints on the cosmological parameters from the product $D_L \cdot DM_{\text{IGM}}$ are independent of the Hubble constant. With the combination of $D_L \cdot DM_{\text{IGM}}$, the propagated error $\sigma_{D_L \cdot DM}$ in $D_L \cdot DM_{\text{IGM}}$ is

$$\sigma_{D_L \cdot DM} = \left[(DM_{\text{IGM}} \cdot \sigma_{D_L})^2 + (D_L \cdot \sigma_{DM_{\text{IGM}}})^2 \right]^{1/2}. \quad (14)$$

In Figure 1, we illustrate the three quantities (D_L , DM_{IGM} , and $D_L \cdot DM_{\text{IGM}}$) as a function of the redshift z in the flat Λ CDM model. To show the sensitivity of the three functions to the cosmological parameter Ω_m , we plot them for five cases of a flat Universe with $\Omega_m = 0.1, 0.3, 0.5, 0.7,$ and 0.9 , relative to an Einstein-de Sitter Universe ($\Omega_m = 1, \Omega_\Lambda = 0$). It is clearly seen that the $D_L \cdot DM_{\text{IGM}}$ curves have a wider separation than the D_L or DM_{IGM} curves to allow a better discrimination among different cosmological models. Meanwhile, the sensitivity increases with the redshift, thus, it is of special significance for the $D_L \cdot DM_{\text{IGM}}$ method to study high-redshift associations.

¹ <http://frbcat.org/>

² <http://www.atnf.csiro.au/research/pulsar/psrcat/>

2.4. Redshifts from electromagnetic counterparts

Measuring the source redshift is crucial when using the GW/FRB association as the upgraded standard siren. Several methods have been suggested to obtain the redshift associated to a GW event, such as the galaxy catalogue (Schutz 1986), NS mass distribution (Marković 1993; Taylor et al. 2012), and the tidal deformation of NSs (Messenger & Read 2012). In this work, we adopt the widely used method of identifying an EM counterpart of the GW event to obtain the source redshift (Nissanke et al. 2010; Sathyaprakash et al. 2010; Zhao et al. 2011). An EM counterpart like the GRB or the kilonova can give the redshift information if the host galaxy of the event can be pinpointed. Besides, the redshift can also be measured from the absorption lines of the GRB afterglows.

3. MONTE CARLO SIMULATIONS

To explore the cosmological constraint ability by future joint measurements of luminosity distance D_L and dispersion measure DM, we perform Monte Carlo simulations on GW/FRB systems. Here we adopt the cosmological parameters of the fiducial flat Λ CDM model derived from *Planck* 2015 data: $H_0 = 67.8 \text{ km s}^{-1} \text{ Mpc}^{-1}$, $\Omega_m = 0.308$, $\Omega_\Lambda = 0.692$, and $\Omega_b = 0.049$ (Planck Collaboration et al. 2016). For the fraction of baryon mass in the IGM, we take $f_{\text{IGM}} = 0.83$ (Fukugita et al. 1998; Shull et al. 2012; Deng & Zhang 2014). If compact binaries are NS–NS binaries or NS–BH binaries, it is believed that the source redshift can be obtained from an EM counterpart that occurs coincidentally with the GW event (Nissanke et al. 2010; Sathyaprakash et al. 2010; Zhao et al. 2011). Moreover, Wang et al. (2016) proposed that possible GW/FRB associations could be detected within the framework of the NS–NS merger model. Therefore, we consider the mergers of binary NS systems as the sources of GWs and FRBs. Following Zhao et al. (2011) and Cai & Yang (2017), the redshift distribution of the sources takes the form

$$P(z) \propto \frac{4\pi D_C^2(z) R(z)}{H(z)(1+z)}, \quad (15)$$

where $D_C(z) = \int_0^z 1/H(z) dz$ is the comoving distance, and $R(z)$ denotes the time evolution of the merger rate and takes the form (Schneider et al. 2001; Cutler & Holz 2009; Cai & Yang 2017)

$$R(z) = \begin{cases} 1+2z, & z \leq 1 \\ \frac{3}{4}(5-z), & 1 < z < 5 \\ 0, & z \geq 5. \end{cases} \quad (16)$$

In our simulations, the redshifts of source z are randomly generated from the redshift probability distribution function (Equation (15)). Since the ET would be able to detect binary NS inspirals up to redshifts of $z \sim 2$, the range of the source redshift z for our analysis is from 0 to 2. With the mock z , we infer the fiducial values of D_L^{fid} and $\text{DM}_{\text{IGM}}^{\text{fid}}$ from Equations (5) and (12), respectively. The mass of each NS and the position angle θ are uniformly distributed in the two parameter intervals: $[1, 2] M_\odot$ and $[0, \pi]$, respectively³. We then calculate the combined SNR of each set of the random sample using Equation (6), and confirm that the simulated signal is a GW detection if $\rho > 8.0$. For every confirmed detection, we add the deviations in Equations (10)

³ We do not need to consider the other two angles ϕ and ψ , since the SNR is independent of them.

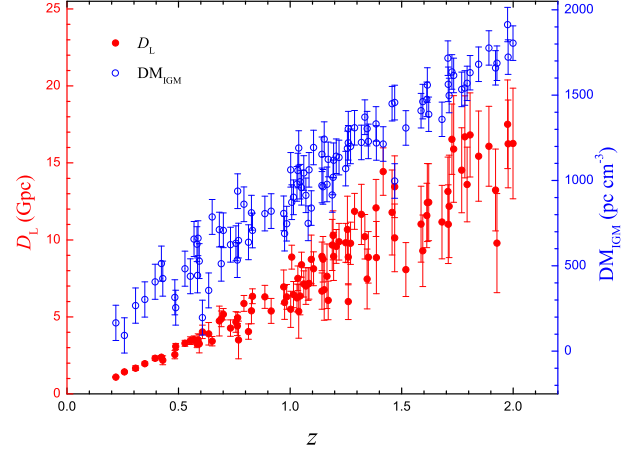


FIG. 2.— An example catalogue of 100 simulated GW/FRB associations with redshifts z , luminosity distances D_L , and dispersion measures DM_{IGM} .

and (13) to the fiducial values of D_L^{fid} and $\text{DM}_{\text{IGM}}^{\text{fid}}$, respectively. That is, we sample the D_L^{mea} (or $\text{DM}_{\text{IGM}}^{\text{mea}}$) measurement according to the Gaussian distribution $D_L^{\text{mea}} = \mathcal{N}(D_L^{\text{fid}}, \sigma_{D_L})$ (or $\text{DM}_{\text{IGM}}^{\text{mea}} = \mathcal{N}(\text{DM}_{\text{IGM}}^{\text{fid}}, \sigma_{\text{DM}_{\text{IGM}}})$). The inferred event rate density of NS–NS mergers from the detection of GW170817 is $\sim 1100_{-910}^{+2500} \text{ Gpc}^{-3} \text{ yr}^{-1}$ (Abbott et al. 2017a). The event rate density of FRBs may be estimated as (Zhang 2016)

$$\dot{\rho}_{\text{FRB}} = \frac{365 \dot{N}_{\text{FRB}}}{(4\pi/3) D_z^3} \simeq (1.4 \times 10^3 \text{ Gpc}^{-3} \text{ yr}^{-1}) \left(\frac{D_z}{3.4 \text{ Gpc}} \right)^{-3} \left(\frac{\dot{N}_{\text{FRB}}}{10^4} \right),$$

where D_z is the comoving distance of the FRB normalized to 3.4 Gpc ($z = 1$), and \dot{N}_{FRB} denotes the daily all-sky FRB rate that is normalized to 10^4 . One can see that the FRB rate is well consistent with the NS–NS merger rate. The expected detection rates of NS–NS and BH–NS per year for the ET⁴ are about the order $10^3 - 10^7$. Taking the detection rate in the middle rang $\mathcal{O}(10^5)$, and assuming that only a small fraction ($\sim 10^{-3}$) of GW/FRB systems could be detected, we can expect to detect $\mathcal{O}(10^2)$ such systems per year. Thus, we simulate a population of 100 GW/FRB systems.

An example of 100 simulated GW/FRB systems from the fiducial model is shown in Figure 2. For a set of 100 simulated data points, the likelihood for the cosmological parameters can be determined by the minimum χ^2 statistic, i.e.,

$$\chi^2(\mathbf{p}) = \sum_i \frac{[D_L^{\text{mea}} \cdot \text{DM}_{\text{IGM}}^{\text{mea}} - D_L^{\text{th}}(\mathbf{p}) \cdot \text{DM}_{\text{IGM}}^{\text{th}}(\mathbf{p})]^2}{\sigma_{D_L \cdot \text{DM}}^2}, \quad (17)$$

where $D_L^{\text{th}} \cdot \text{DM}_{\text{IGM}}^{\text{th}}$ is the theoretical value calculated from the set of cosmological parameters \mathbf{p} . Similar expressions are computed for the methods of D_L and DM_{IGM} . This simulation is repeated for 1000 times to ensure the final constraint results are unbiased.

In w CDM, the equation-of-state of dark energy, w , is constant, and there are three free parameters: Ω_m , w , and H_0 . It should be underlined that the $D_L \cdot \text{DM}_{\text{IGM}}$ method (the product of Equations (5) and (12)) can be used to test cosmological models in a rather unique way because, unlike the other two methods (D_L or DM_{IGM}) that rely on the optimization of the Hubble constant H_0 , this particular analysis is completely independent of H_0 . For the D_L and DM_{IGM} methods, we let Ω_m

⁴ The Einstein Telescope Project, <https://www.et.gw.eu/et/>.

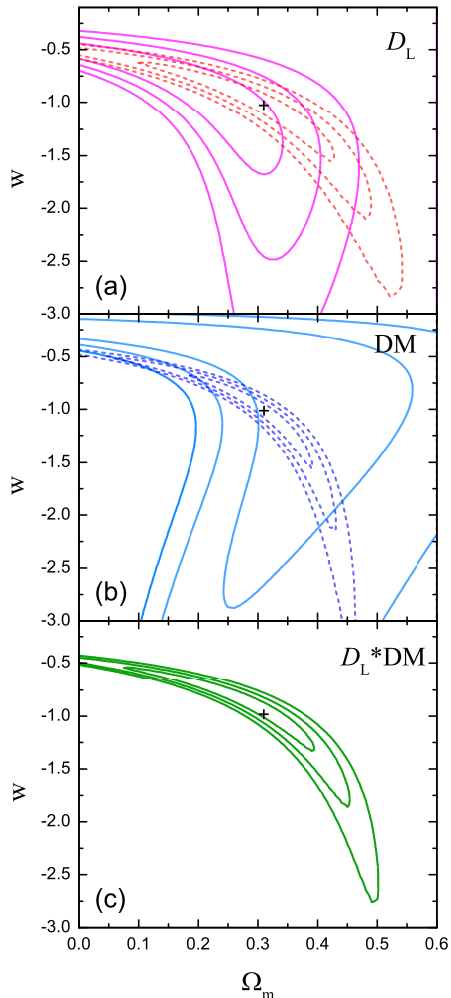


FIG. 3.— Constraint results of (Ω_m, w) in the w CDM model from 100 simulated GW/FRB systems using three different methods (from top to bottom): D_L , DM_{IGM} , and $D_L \cdot DM_{\text{IGM}}$. Unlike the methods of D_L and DM_{IGM} that rely on the optimization of H_0 , the $D_L \cdot DM_{\text{IGM}}$ method is independent of H_0 . The dashed and solid contours in panels (a) and (b) correspond to the cases of fixing and marginalizing over H_0 , respectively. The plus symbols denote the simulated values.

and w to be free parameters while either fixing or marginalizing over H_0 .

We first marginalize H_0 in the w CDM model to find the confidence levels in the $\Omega_m - w$ plane. The constraint results (solid lines) from three different methods (D_L , DM_{IGM} , and $D_L \cdot DM_{\text{IGM}}$) are illustrated in Figure 3. One can see from these solid contours that the $D_L \cdot DM_{\text{IGM}}$ method gives much tighter constraints on both cosmological parameters than the other two methods as we expected. In both the traditional standard-siren approach (i.e., the D_L method) and the DM_{IGM} method, we need a much larger sample to increase the significance of the constraints. In contrast, future observations of GWs and their FRB counterparts will enable us to achieve precise cosmography from around 100 such systems. All in all, upgraded standard sirens could be constructed if GW/FRB association systems are commonly detected in the future.

To show the importance of H_0 in the D_L and DM_{IGM} methods, we also present the case of fixing $H_0 = 67.8 \text{ km s}^{-1} \text{ Mpc}^{-1}$. As shown by the dashed contours in Figures 3(a) and (b), the constraints on cosmological parameters can be signif-

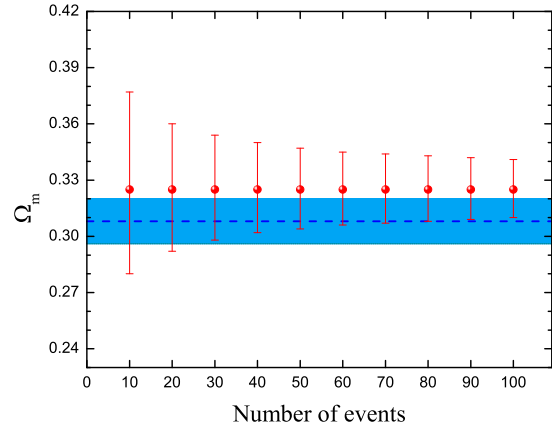


FIG. 4.— The best-fit Ω_m (red dot) and 1σ confidence level (red line) in the flat Λ CDM model as a function of the number of GW/FRB associations. The dashed line is the fiducial value. The blue shaded area represents the 1σ confidence level constraint from Planck 2015 results.

icantly improved when H_0 is fixed. Even if the prior value of H_0 is adopted, however, the constraints obtained from the methods of D_L and DM_{IGM} are still not better than that of the $D_L \cdot DM_{\text{IGM}}$ method (Figure 3c). Therefore, we can conclude that the cosmological constraint ability of the methods of D_L and DM_{IGM} are restricted by the fact that they both explicitly depend on H_0 , while the $D_L \cdot DM_{\text{IGM}}$ method has the advantage of being independent of H_0 .

To better represent how effective this $D_L \cdot DM_{\text{IGM}}$ method might be with a certain number of coincident detections, in Figure 4 we plot the best-fit dark matter density parameter Ω_m and 1σ confidence level in the flat Λ CDM model as a function of the number of GW/FRB associations (analogous to Figure 5 of Del Pozzo (2012)). The 1σ confidence level constraint on Ω_m from Planck temperature data and Planck lensing combined results (blue shaded area; Planck Collaboration et al. 2016) is also plotted for comparison. One can see from this figure that with about 100 GW/FRB associations we can constrain Ω_m with an accuracy comparable to Planck data.

4. SUMMARY AND DISCUSSION

In this work, we propose that if GW/FRB associations are confirmed to commonly exist, upgraded standard sirens can be constructed from the joint measurements of luminosity distances D_L derived from GWs and dispersion measures DM_{IGM} derived from FRBs. Moreover, the combination of D_L and DM_{IGM} (i.e., the $D_L \cdot DM_{\text{IGM}}$ method) can be used to differentiate cosmological models in a rather unique way because, unlike the traditional standard-siren approach (i.e., the D_L method) and the DM_{IGM} method that rely on the optimization of the Hubble constant H_0 , this particular analysis is completely independent of H_0 . Through Monte Carlo simulations, we prove that this $D_L \cdot DM_{\text{IGM}}$ method is able to constrain the cosmological parameters more strongly than D_L or DM_{IGM} separately. With the help of the $D_L \cdot DM_{\text{IGM}}$ method, precise multimessenger cosmology can be achieved from around 100 GW/FRB systems.

Thanks to the high sensitivity, the planned third-generation GW detectors, such as the ET, could detect about $10^3 - 10^7$ NS-NS and BH-NS merger GW events per year. Although a considerable catalogue of GW events would be obtained, the measurements of GW/FRB association systems suggested by

our method may not be easy in practice. To be specific, only in the optimistic case that satisfying (i) GWs and FRBs are confirmed to have the same progenitor system; (ii) the coincident detections of GW events with FRBs can be accomplished by the collaboration of the GW interferometric detectors and the radio transient surveys; (iii) the source redshifts can be identified; (iv) an overall statistical error from the contribution of DM_{obs} , DM_{MW} , and DM_{HG} is smaller than the systematic uncertainty σ_{IGM} in modeling and inferring the dispersion measure DM_{IGM} of the intergalactic plasma,⁵ and σ_{IGM} is not too big, GW/FRB systems could serve as a viable cosmic probe. If some of these requirements are not met, the using of GW/FRB systems as upgraded standard sirens would be challenged. Although in this work we just discuss FRBs, the methodology developed here is also applicable for any other kinds of cosmological radio transients that occur simultaneously with GWs, if there are, to constrain the cosmological parameters and the equation of state of dark energy with high

accuracy. On the other hand, even if FRBs are not associated with GWs, our method is still applicable for those GWs and FRBs that occur at the same redshifts.

We thank the anonymous referee for constructive suggestions. This work is partially supported by the National Basic Research Program (“973” Program) of China (Grant No. 2014CB845800), the National Natural Science Foundation of China (Grant Nos. 11603076, 11673068, and 11725314), the Youth Innovation Promotion Association (2011231 and 2017366), the Key Research Program of Frontier Sciences (Grant No. QYZDB-SSW-SYS005), the Strategic Priority Research Program “Multi-waveband gravitational wave Universe” (Grant No. XDB23000000) of the Chinese Academy of Sciences, and the Natural Science Foundation of Jiangsu Province (Grant No. BK20161096).

REFERENCES

- Abbott, B. P., Abbott, R., Abbott, T. D., et al. 2017a, *Physical Review Letters*, 119, 161101
- Abbott, B. P., Abbott, R., Abbott, T. D., et al. 2017b, *Nature*, 551, 85
- Anderson, L., Aubourg, E., Bailey, S., et al. 2012, *MNRAS*, 427, 3435
- Beutler, F., Blake, C., Colless, M., et al. 2011, *MNRAS*, 416, 3017
- Cai, R.-G., Cao, Z., Guo, Z.-K., Wang, S.-J., & Yang, T. 2017, *Natl. Sci. Rev.*, 4, 687
- Cai, R.-G., & Yang, T. 2017, *Phys. Rev. D*, 95, 044024
- Coulter, D. A., Foley, R. J., Kilpatrick, C. D., et al. 2017, *Science*, 358, 1556
- Cutler, C., & Holz, D. E. 2009, *Phys. Rev. D*, 80, 104009
- Del Pozzo, W. 2012, *Phys. Rev. D*, 86, 043011
- Del Pozzo, W., Li, T. G. F., & Messenger, C. 2017, *Phys. Rev. D*, 95, 043502
- Deng, W., & Zhang, B. 2014, *ApJ*, 783, L35
- Fan, X., Carilli, C. L., & Keating, B. 2006, *ARA&A*, 44, 415
- Fernández, R., & Metzger, B. D. 2016, *Annual Review of Nuclear and Particle Science*, 66, 23
- Fukugita, M., Hogan, C. J., & Peebles, P. J. E. 1998, *ApJ*, 503, 518
- Gao, H., Li, Z., & Zhang, B. 2014, *ApJ*, 788, 189
- Goldstein, A., Veres, P., Burns, E., et al. 2017, *ApJ*, 848, L14
- Hinshaw, G., Larson, D., Komatsu, E., et al. 2013, *ApJS*, 208, 19
- Holz, D. E., & Hughes, S. A. 2005, *ApJ*, 629, 15
- Lorimer, D. R., Bailes, M., McLaughlin, M. A., Narkevic, D. J., & Crawford, F. 2007, *Science*, 318, 777
- Manchester, R. N., Hobbs, G. B., Teoh, A., & Hobbs, M. 2005, *AJ*, 129, 1993
- Marković, D. 1993, *Phys. Rev. D*, 48, 4738
- McQuinn, M., Lidz, A., Zaldarriaga, M., et al. 2009, *ApJ*, 694, 842
- Messenger, C., & Read, J. 2012, *Physical Review Letters*, 108, 091101
- Mingarelli, C. M. F., Levin, J., & Lazio, T. J. W. 2015, *ApJ*, 814, L20
- Nissanke, S., Holz, D. E., Hughes, S. A., Dalal, N., & Sievers, J. L. 2010, *ApJ*, 725, 496
- Perlmutter, S., Aldering, G., della Valle, M., et al. 1998, *Nature*, 391, 51
- Petroff, E., Barr, E. D., Jameson, A., et al. 2016, *PASA*, 33, e045
- Planck Collaboration, Ade, P. A. R., Aghanim, N., et al. 2016, *A&A*, 594, A13
- Riess, A. G., Filippenko, A. V., Challis, P., et al. 1998, *AJ*, 116, 1009
- Sathyaprakash, B. S., & Schutz, B. F. 2009, *Living Reviews in Relativity*, 12, 2
- Sathyaprakash, B. S., Schutz, B. F., & Van Den Broeck, C. 2010, *Classical and Quantum Gravity*, 27, 215006
- Savchenko, V., Ferrigno, C., Kuulkers, E., et al. 2017, *ApJ*, 848, L15
- Schneider, R., Ferrari, V., Matarrese, S., & Portegies Zwart, S. F. 2001, *MNRAS*, 324, 797
- Schutz, B. F. 1986, *Nature*, 323, 310
- Shull, J. M., Smith, B. D., & Danforth, C. W. 2012, *ApJ*, 759, 23
- Taylor, S. R., Gair, J. R., & Mandel, I. 2012, *Phys. Rev. D*, 85, 023535
- Thornton, D., Stappers, B., Bailes, M., et al. 2013, *Science*, 341, 53
- Totani, T. 2013, *PASJ*, 65, L12
- Wang, J.-S., Yang, Y.-P., Wu, X.-F., Dai, Z.-G., & Wang, F.-Y. 2016, *ApJ*, 822, L7
- Yamasaki, S., Totani, T., & Kiuchi, K. 2017, *ArXiv e-prints*, arXiv:1710.02302
- Yang, Y.-P., & Zhang, B. 2016, *ApJ*, 830, L31
- Zhang, B. 2016, *ApJ*, 827, L31
- Zhao, W., van den Broeck, C., Baskaran, D., & Li, T. G. F. 2011, *Phys. Rev. D*, 83, 023005
- Zheng, Z., Ofek, E. O., Kulkarni, S. R., Neill, J. D., & Juric, M. 2014, *ApJ*, 797, 71
- Zhou, B., Li, X., Wang, T., Fan, Y.-Z., & Wei, D.-M. 2014, *Phys. Rev. D*, 89, 107303

⁵ If it turns out that the statistical error could become larger than σ_{IGM} , the

accuracy of our results would be reduced dramatically.